

RECENT DEVELOPMENTS IN RELATIVISTIC MODELS FOR EXCLUSIVE $A(e, e'p)B$ REACTIONS

J.M. Udías,^{1,†} Javier R. Vignote,¹ E. Moya de Guerra,² A. Escuderos,² and J.A. Caballero³

¹*Dpto. Física Atómica, Molecular y Nuclear, Universidad Complutense de Madrid, Spain*

²*Instituto de Estructura de la Materia (CSIC), Madrid, Spain*

³*Dpto. Física Atómica, Molecular y Nuclear, Universidad de Sevilla, Spain*

A comparison of impulse approximation calculations for the $(e, e'p)$ reaction, based on the Dirac equation and the Schrödinger one is presented. Trivial (kinematics) differences are indicated, as well as how to remove them from the standard nonrelativistic formalism. Signatures of the relativistic approach are found where the enhancement of the lower components (spinor distortion or negative energy contributions) modifies TL observables with respect to the nonrelativistic predictions, what seems to be confirmed by the experiment. Finally, the relativistic approach is used to analyze several experiments for the reaction $^{16}O(e, e'p)^{15}N$ taken at values of Q^2 from 0.2 to 0.8 $(GeV/c)^2$, not finding a significant Q^2 dependence of the scale factors over this range.

1. INTRODUCTION

Quasielastic $(e, e'p)$ processes are a powerful tool to study bound nucleon properties. Indeed, coincidence $(e, e'p)$ measurements at quasielastic kinematics have provided over the years detailed information on the energies, momentum distributions and spectroscopic factors of bound nucleons. This is so because at quasielastic kinematics the $(e, e'p)$ reaction can be treated with confidence in the impulse approximation, *i.e.*, assuming that the detected proton absorbs the whole momentum (q) and energy (ω) of the exchanged photon (for recent reviews of the subject see ref. [1] and references therein). Until recently, most data were concentrated in the low missing momentum range $p_m \leq 300$ MeV/c, where p_m is the recoil momentum of the residual nucleus. In the last years [2] higher p_m -regions are being probed at small missing energies (E_m) to study further aspects of bound nucleon dynamics and nucleon currents.

The higher momentum transfer employed in the new experiments, made almost compulsory a fully relativistic treatment of the reaction mechanism. Within the most simple relativistic framework, that parallels usual nonrelativistic approaches, a single-particle equation is used to compute both the bound and ejected nucleon wave function. The difference between the nonrelativistic approach employed in the 70's and 80's and the relativistic formalism lies thus, mainly, in the use of the Dirac equation instead of the Schrödinger one. The success of the simple Dirac single-particle picture in describing detailed features of the $(e, e'p)$ experimental data is intriguing and deserves close examination. In this contribution we compare in detail the nonrelativistic and relativistic impulse approximation to $(e, e'p)$.

2. FORMALISM

In the relativistic distorted wave impulse approximation (RDWIA)[3, 4, 5, 6, 7, 8, 9] the one-body nucleon current, written for convenience in p -space,

$$J_N^\mu(\omega, \vec{q}) = \int d\vec{p} \bar{\psi}_F(\vec{p} + \vec{q}) \hat{J}_N^\mu(\omega, \vec{q}) \psi_B(\vec{p}), \quad (1)$$

is calculated with relativistic ψ_B and ψ_F wave functions for initial bound and final outgoing nucleons, respectively, and with relativistic nucleon current operator, \hat{J}_N^μ . The bound state wave function is a four-spinor with well-defined parity and angular momentum quantum numbers, and

[†]Electronic address: jose@nuc2.fis.ucm.es; URL: <http://nuclear.fis.ucm.es>

is obtained by solving the Dirac equation with scalar-vector (S-V) potentials determined through a Hartree procedure from a relativistic Lagrangian with scalar and vector meson terms [10]. The wave function for the outgoing proton is a solution of the Dirac equation containing S-V global optical potentials [11] for a nucleon scattered with asymptotic momentum \vec{P}_F . Dirac equations for both scattered and bound wave functions are solved in coordinate space and their solutions are then transformed to momentum space where necessary.

Eq. (1) sets up the scenario where differences between the relativistic and nonrelativistic impulse approximation approaches are at play. As a guide in the comparison with the nonrelativistic formalism we study the so-called *factorized approximation*, not because it is often used (nowadays the simple factorized results are hardly employed to analyze exclusive $(e, e'p)$ experiments) but because of its simplicity and usefulness as a pedagogical tool.

A Factorization

The $(e, e'p)$ reaction has a simple interpretation if one assumes a factorized expression for the cross-section, *i.e.*:

$$\frac{d^5\sigma}{d\Omega_e d\varepsilon' d\Omega_F} = K \sigma_{ep} S(E_m, \vec{p}_m) \quad (2)$$

where K is the phase-space factor, σ_{ep} is the electron-proton cross-section and $S(E_m, \vec{p}_m)$ is the *spectral function* representing the probability of finding a proton in the target nucleus with missing energy E_m and missing momentum p_m , compatible with the kinematics of the reaction. Distortion of the electron wave functions due to the Coulomb potential as well as of the nucleon wave functions, break the factorized approach at the level of cross-sections. Due to this, most calculations of exclusive $(e, e'p)$ cross-sections are performed within a fully unfactorized approach. Within the impulse approximation, the cross-section is computed from the contraction of the electron current with the nuclear current matrix element of eq. (1). We recall now a relevant example.

B Matrix element of the electromagnetic current for free nucleons

Let's assume for a moment that we compute the matrix element in eq. (1) using free spinors with momenta identical to the asymptotic momenta of the nucleon (initial \vec{p}_m , final \vec{P}_F), so that the resulting nuclear matrix element reads (omitting for the moment the spin indices):

$$J_{N,\text{free}}^\mu(\omega, \vec{q}, \vec{P}_F, \vec{p}_m) = \delta(\vec{P}_F - \vec{p}_m - \vec{q}) \bar{u}(\vec{P}_F) \hat{J}_N^\mu(\omega, \vec{q}) u(\vec{p}_m). \quad (3)$$

In previous expression, 4-spinors and 4×4 Dirac operators are involved. Besides, a momentum-conserving delta function appears so that, in the computation of this matrix element, the momenta of the initial and final nucleon are related by $\vec{p}_m = \vec{P}_F - \vec{q}$.

Now we note that the previous expression eq. (3) can be recast in a way that only Pauli spinors appear explicitly:

$$J_{N,\text{free}}^\mu(\omega, \vec{q}, \vec{P}_F, \vec{p}_m) = \delta(\vec{P}_F - \vec{p}_m - \vec{q}) \chi^{\sigma_F \dagger} \hat{J}_{2 \times 2}^{eff}(\text{free}, \omega, \vec{q}, \vec{P}_F, \vec{p}_m) \chi^{\sigma_i} \quad (4)$$

The effective 2×2 current operator makes the bridge from the 4×4 matrix expression to the one suitable for a nonrelativistic calculation. Explicit expressions for the nontruncated operator $\hat{J}_{2 \times 2}^{eff}(\text{free})$ can be found in many references, for instance in [12, 13]. Otherwise, both expressions eq. (1) and eq. (4) are completely equivalent *for free spinors* in order to compute the amplitude at the nucleon vertex. For instance, the elementary electron-proton cross-section σ_{ep} of eq. (2) will typically be computed from the matrix element of eq. (3) or equivalently eq. (4). The σ_{ce1} of de Forest is computed this way [14].

If an operator different from $\hat{J}_{2 \times 2}^{eff}(\text{free}, \omega, \vec{q}, \vec{P}_F, \vec{p}_m)$ is employed to compute the $(e, e'p)$ cross-section, factorization will obviously be lost, already at the level of the nuclear matrix element. An

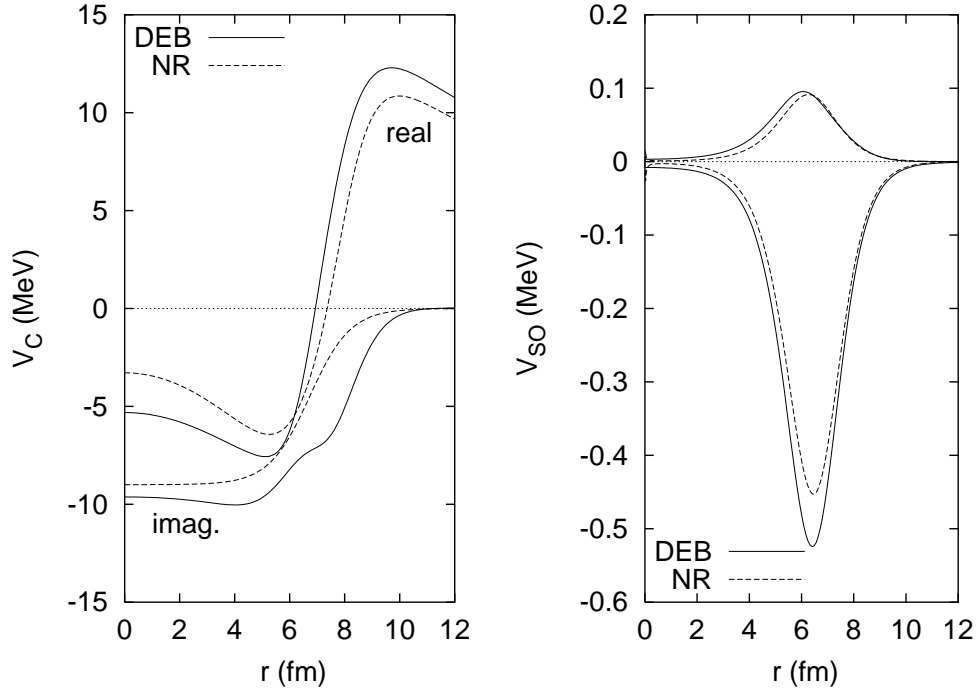


FIG. 1: Comparison of standard nonrelativistic (NR) central and spin-orbit potentials for ^{208}Pb at $T' = 100$ MeV taken from ref. [16] and the potentials V_C , V_{SO} derived with the Dirac equation based (DEB) procedure of eq. (12) from a typical relativistic set of S-V potentials from ref. [11].

example: in typical nonrelativistic calculations [15], $\hat{J}_{2 \times 2}^{eff}(\text{free}, \omega, \vec{q}, \vec{P}_F, \vec{p}_m)$ is expanded in powers of \vec{p}_m/M and as a consequence the matrix element obtained with this truncated operator will yield numerically different results from the one in eq. (3) or eq. (4), *even when sandwiched between free spinors*. This kind of difference between a nonrelativistically truncated operator and $\hat{J}_{2 \times 2}^{eff}(\text{free}, \omega, \vec{q}, \vec{P}_F, \vec{p}_m)$ is what we term *kinematical* (trivial) relativistic effects. These differences can be avoided by using the full $\hat{J}_{2 \times 2}^{eff}(\text{free})$.

C Further (nontrivial) differences between relativistic and nonrelativistic matrix elements

According to the (relativistic) IA, to compute the nuclear matrix element for the $(e, e'p)$ process, we substitute in eq. (1) the free spinors by 4-spinor solutions of Dirac equation. Or alternatively, in the (nonrelativistic) IA, we start from eq. (4) and we substitute the free Pauli spinors by solutions of the Schrödinger equation. This introduces two kinds of numerical differences between approaches based on eq. (1) and eq. (4) what we call *dynamical* differences:

1. The lower component of the 4-spinor solutions of Dirac equation are not related to the upper ones by the same relationship (free Dirac equation) that holds for free spinors and that is implicitly assumed in the derivation of $\hat{J}_{2 \times 2}^{eff}(\text{free}, \omega, \vec{q}, \vec{P}_F, \vec{p}_m)$.
2. The upper component of the solutions of Dirac equation are different from the solutions of Schrödinger one, even if equivalent potentials (that lead to the same binding energy and phase-shifts) are used in both equations.

We shall first focus on this second point. We usually start from the Dirac equation:

$$(\tilde{E}\gamma_0 - \vec{p} \cdot \vec{\gamma} - \tilde{M})\psi = 0 \quad (5)$$

with S and V spherically symmetric potentials,

$$\tilde{E} = E - V(r) \quad (6)$$

$$\tilde{M} = M - S(r) \quad (7)$$

$$\psi = \begin{pmatrix} \psi_{up} \\ \psi_{down} \end{pmatrix}, \quad (8)$$

This equation can be written either as a system of coupled linear differential equations for ψ_{up} , ψ_{down} , or as a second order differential Schrödinger like-equation for ψ_{up} :

$$\left[\frac{-\vec{\nabla}^2}{2M} - U_C - U_{LS}\vec{\sigma} \cdot \vec{\ell} + \frac{1}{2MrA(r)} \frac{dA(r)}{r} \vec{r} \cdot \vec{\nabla} \right] \psi_{up}(\vec{r}) = 0 \quad (9)$$

Due to the linear term $\vec{\nabla}$ (Darwin term), previous equation is not yet quite a Schrödinger-like equation. Using the standard transformation

$$\psi_{up}(r) = K(r)\phi(r), \quad (10)$$

the non-local (Darwin) term can be eliminated to obtain a more standard Schrödinger equation with second derivatives only

$$\left[\frac{-\vec{\nabla}^2}{2M} - U_{DEB} \right] \phi(\vec{r}) = \frac{(E^2 - M^2)}{2M} \phi(\vec{r}) \quad (11)$$

$$\begin{aligned} U_{DEB} &= V_C + V_{SO} \vec{\sigma} \cdot \vec{\ell} \\ V_C &= \frac{1}{2M} [V^2 - 2EV - S^2 + 2MS + V_D] \\ V_D &= \frac{1}{rA} \frac{\partial A}{\partial r} + \frac{1}{2A} \frac{\partial^2 A}{\partial r^2} - \frac{3}{4A^2} \left(\frac{\partial A}{\partial r} \right)^2 \\ V_{SO} &= \frac{1}{2M} \frac{1}{rA} \frac{\partial A}{\partial r} \\ A(r) &= \frac{\tilde{E} + \tilde{M}}{E + M} = K^2(r). \end{aligned} \quad (12)$$

The former set of equations eqs. (11), (12) defines the Schrödinger-like equation and the Dirac equation based (DEB) potentials. Eq. (11) is formally identical to the usual Schrödinger equation, and actually several groups use or have used this analogy to compute the full solution of the Dirac formalism taking advantage of computational tools for nonrelativistic equations [17, 18].

A comparison of V_C and V_{SO} taken from the phenomenology with a nonrelativistic approach or with the relativistic one after a DEB procedure, shows that these potentials are very similar, as depicted in Fig. 1. After careful inspection of the equations, three remarks are however in order:

1. The solution of the Schrödinger-like equation, even though being phase-shift and energy eigenvalue equivalent to the solution of the original Dirac equation, is not identical to the upper component of the initial Dirac equation. It differs from it by the Darwin factor given by eqs. (10,12).
2. The central potential V_C (DEB) has a linear dependence on the energy. That is, it is strongly nonlocal. Disregarding V_D that is usually negligible, it is clear from previous eqs. (12) that, even if V and S potentials of the Dirac equation were energy independent, V_C (DEB) is not.
3. The lower component of the full 4-spinor solution of Dirac equation is absent in the Schrödinger-like approach.

We now study more in detail points 1 and 2.

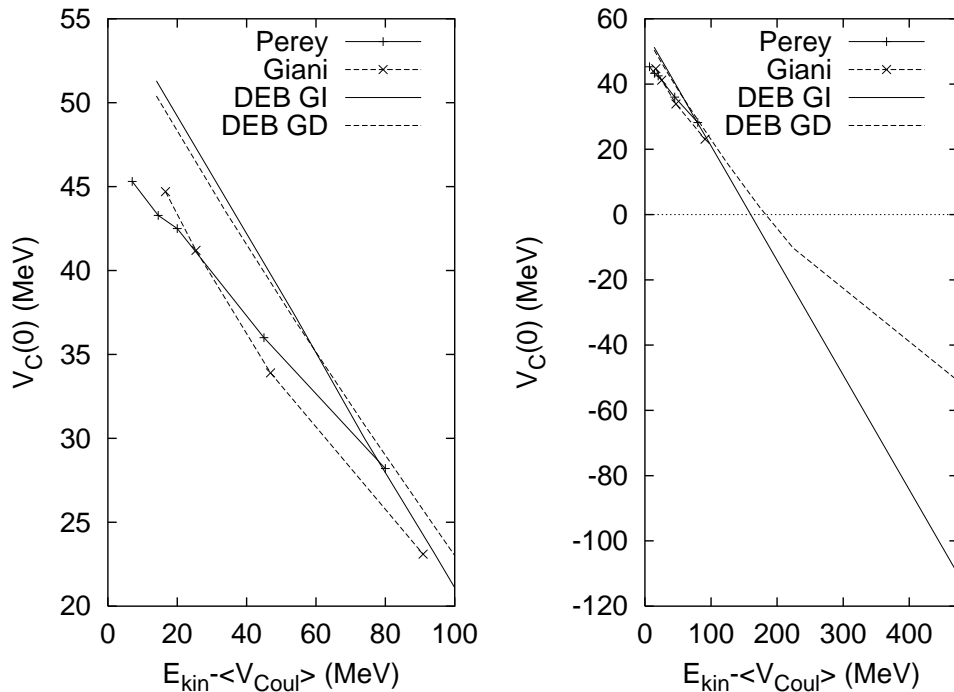


FIG. 2: Depth at the origin of the local potential extracted from non-relativistic analyses of elastic nucleon scattering in ^{208}Pb at two different ranges of kinetic energy of the scattered nucleon. Results from the well-known works of Perey *et al.* [20] and Gianini *et al.* [21] are compared to the dependence found in V_C (DEB) taken from the S-V potentials of Clark *et al.* [11] at $T' = 100$ MeV (DEB GI) and for the energy dependent relativistic parameterization (DEB GD).

D Nonlocality and quenching of the upper components

In the early times, it was found in analyses of nucleon-nucleus reactions based on the Schrödinger equation with a local optical potential, that this potential has a strong dependence on the energy of the nucleon. This was attributed to the fact that a fully nonlocal Schrödinger equation should be used instead of the local one given by eq. (11). The solutions of the local and the nonlocal Schrödinger equation are related by a nonlocality factor [19, 20, 21], in very much the same way the Darwin factor relates the upper component of Dirac equation to the solution of the DEB Schrödinger equation.

In Fig. 2 the energy dependence of several local optical potentials is shown, along with the one of V_C (DEB). These local potentials were fitted to elastic nucleon scattering observables. In the case of the DEB ones, they were obtained from the S-V potentials of ref. [11], in one case neglecting the additional energy dependence of the relativistic potentials, that is, introducing in eq. (12) the S and V potentials for a fixed kinetic energy of 100 MeV (DEB GI), and in the other case (DEB GD) the rather soft dependence of the S, V potentials is included, thus in eq. (12), besides from the explicit linear dependence on E, we also have $S(E)$ and $V(E)$, the energy dependence of the S and V potentials. This additional energy dependence is only visible if a large range of kinetic energy is chosen, as done in the right panel of Fig. (2). On the other hand, as shown in the left panel, for a small range of kinetic energies, the dominant dependence on the energy of the DEB potential is just the linear one explicitly seen in eq. (12).

Also we quote in Table I the parameters of the nonlocal potential (but energy independent) that leads to same elastic proton scattering observables than the local one (but energy dependent), as well as the ones that result when a nonlocality analyses of the Perey kind [20] is done to the DEB potentials. The nonlocality range of the potential is similar in all cases, (β_{nl}) in between 0.82 and

	particle	energy range	V_{nl}^o (MeV)	β_{nl} (fm)
Perey and Buck (1961)[20]	n	7-14.5 MeV	-71	0.85
Giannini and Rico (1976)[21]	n,p	70-150	-89	0.95
Schwandt (1982)[22]	p	80-150	-75	0.82
Clark GI	p	60	-150	0.95
Clark GD	p	22-1024	-110	1.0

TABLE I: Nonlocality parameters of the Perey-Buck kind [20] derived from optical potential analyses of elastic nucleon-nucleus scattering. The depth V_{nl}^o and nonlocality range of the nonlocal (energy independent) potential equivalent to the local (energy dependent) one are quoted. Last two rows show what we find if the same analysis is done to the V_C potentials of the DEB procedure from the S-V potentials of Clark et al. at $T' = 100$ MeV (GI), and for the EDAI parameterization (GD) [11].

1.0 fm.

A larger value of the nonlocality range implies a Perey factor more different from one. The shape of the Perey factor and that of the Darwin factor is very similar (for instance the Darwin factor can be seen in Fig. 3) More remarkably, if one considers a DEB potential and builds the Perey factor from the linear energy dependence displayed by the potential, then this factor is practically equal to the Darwin factor needed to make the solution of the Schrödinger-like equation ϕ in eq. (11) equal to the upper component of the solution of the initial Dirac equation [4]. This very striking equivalence has been studied in high detail in [4, 19, 23].

Thus, the situation is such that the nonlocal nature of the optical potential seen in the nonrelativistic analyses could very well be a way of implementing the relativistic features of Dirac equation. But also perhaps the other way around!. Only with elastic observables it is not possible to disentangle between these two (nonlocality of the Perey kind *versus* Darwin factor from Dirac equation) aspects, as they are not sensitive to the inner part of the wave function. ($e, e'p$) experiments on the other hand, do sample the nuclear interior where either the Darwin or the Perey factor reduce the nucleon density. This yields smaller cross-section and thus has an effect in scale factors [3, 4]. However, given this equivalence between Perey and Darwin factors (at least for intermediate nucleon energies) both relativistic and nonrelativistic approaches would be also impossible to disentangle attending only to cross-sections or scale factors derived from ($e, e'p$) experiments. As we will see later, perhaps other observables different from cross-sections will be of help.

A few additional comments: a) The Darwin or Perey term controversy could in principle be also present for the bound state wave function. However, the shape of the Darwin term is almost flat (see Fig. 3) except at the nuclear surface, where it goes to one. Taking into account that the bound state is normalized to one in the nuclear volume, the effect of an almost constant factor inside this nuclear volume, as it is the case of the Perey or Darwin ones, is negligible. Recall that, on the other hand, the scattering states are normalized by comparing their asymptotical behavior with the one of free waves, that is, in a region where both the Perey and the Darwin factor are equal to one and thus the normalization procedure does not affect them. b) Even though the Perey kind of nonlocality associated to a linear dependence in the energy of the potentials is the dominant one, it is possible that additional nonlocalities should be considered. We refer the reader to ref. [19] for a detailed account of the comparison of extended nonlocality nonrelativistic approaches and the relativistic one.

E Enhancement of the lower components

So far, there is one important difference between relativistic and nonrelativistic approaches that remains to be studied, namely the lower components of the Dirac equation solution. Nonrelativistic formalisms are based on the effective 2×2 operator $\hat{J}_{2 \times 2}^{eff}(\text{free}, \omega, \vec{q}, \vec{P}_F, \vec{p}_m)$ derived after making some sort of assumption about the lower components, most often, that they are given by the same relation that holds for free spinors. This assumption is also made in computing σ_{ep} of eq. (2), and thus it is a prerequisite for a factorized calculation. For a general solution of Dirac equation we have:

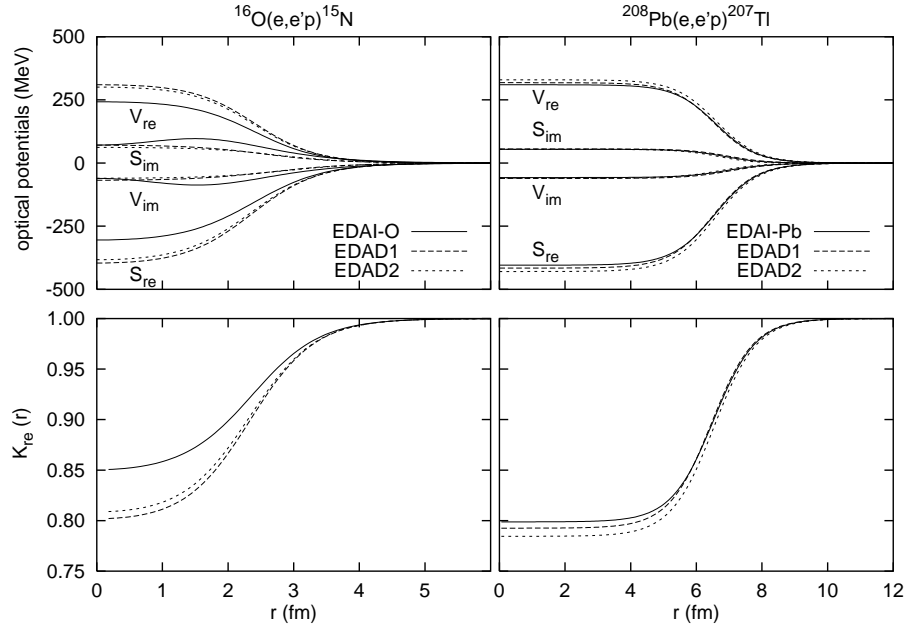


FIG. 3: Upper panels: relativistic S-V optical potentials for ^{15}N (left) and ^{207}Tl (right) at $T' = 100$ MeV, from three different parameterizations. Lower panels: Darwin factors associated to the relativistic optical potentials. Only the real part of the Darwin term is shown, the imaginary one is negligible. We see that, while for ^{207}Tl the A-dependent (EDAD-1 or EDAD-2) and A-independent parameterization of the potentials lead to very similar results. However, for ^{15}N there are noticeable differences both in the potentials and the Darwin term. These differences translate in a large variation of the scale factor derived from the A-independent and the A-dependent potentials for the reaction $^{16}\text{O}(e, e'p)^{15}\text{N}$ (see Fig. 7).

$$\psi_{down} = \frac{\vec{\sigma} \cdot \vec{p}}{\tilde{E} + \tilde{M}} \psi_{up}, \quad (13)$$

for a free nucleon $\tilde{M} = M$, $\tilde{E} = E$, but in a Dirac equation with typical standard potentials, we have $\tilde{E} + \tilde{M} \simeq 0.5(E + M)$ thus the lower components are *enhanced* with respect to the free case. Due to this, matrix elements of eq. (1) have a different behaviour than the ones of eq. (3) and thus the *matrix element* does not factorize into a *free part* dealing only with free spinors (positive energy solutions) and the nucleon momentum distribution (see for details refs. [24, 25]). Thus factorization is broken even before summing and averaging in spins and integrating into the bound nucleon momentum to obtain the matrix element. This is quite different from the nonrelativistic case where there is always factorization at the level of the matrix element, that is, before the integration in \vec{p} of the bound nucleon and summing and averaging of spins, provided that the same operator $\hat{J}_{2 \times 2}^{eff}(\text{free}, \omega, \vec{q}, \vec{P}_F, \vec{p}_m)$ is used to compute $\sigma(e, e'p)$ and σ_{ep} . As it is well known [1] in the nonrelativistic IA, the spin-orbit part of the optical potential for instance breaks factorization at the level of the cross-section (after summing and averaging over spins). Thus if no FSI effects are considered (using plane waves for the final nucleon), factorization may be recovered in the nonrelativistic IA. However, as we have just mentioned, factorization is broken in the relativistic case even if no FSI are included in the calculation [24]. This *strong* breakdown of factorization in the relativistic case is due to the enhancement of the lower components with regards

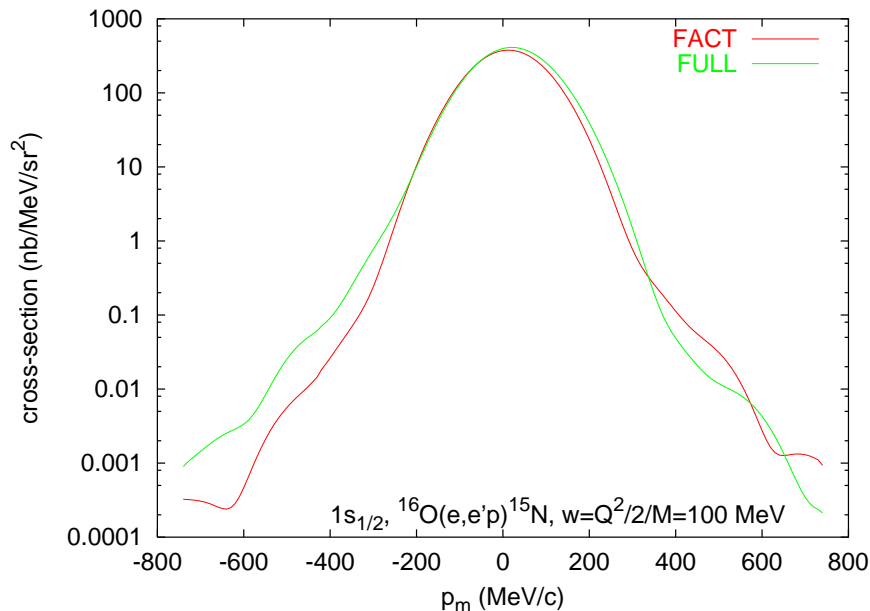


FIG. 4: Cross-section for the $^{16}\text{O}(e, e'p)^{15}\text{N}$ reaction. The full calculation is compared with the factorized result.

to the free case and should translate into differences in the $(e, e'p)$ observables. In particular the relativistically computed cross-sections should depart *more strongly* from the factorized result than the nonrelativistic one.

As shown in Fig. 4 factorization is a good estimate of the ‘bulk’ of the cross-section, at least for quasielastic kinematics. A breakdown of the factorization would be easier to see measuring partial contributions to the cross-section, and comparing them to the L , T and TL contributions to σ_{ep} . Factorization means that the reduced spectral function ρ :

$$\rho = \frac{d^5\sigma(e, e'p)}{d\Omega_e d\Omega_F d\varepsilon'} (K\sigma_{ep})^{-1} \quad (14)$$

would be the identical if derived from the total contribution to both the $(e, e'p)$ cross-section in the numerator and the electron-proton one in the denominator, or only the T , L , TL or any other individual contribution to the cross-section. Now, instead of comparing partial contributions to the reduced cross-sections (or the response functions R^L, R^T, R^{TL}), it will be better to compare ratios of cross-sections, that are independent on the scale-factor, and thus would clearly display any departure from the factorized result. In particular the TL asymmetry A_{TL} given by

$$A_{TL} = \frac{\sigma(\phi_F = 180^\circ) - \sigma(\phi_F = 0^\circ)}{\sigma(\phi_F = 180^\circ) + \sigma(\phi_F = 0^\circ)}. \quad (15)$$

is very adequate. In Fig. 5 this observable is displayed for the $1s_{1/2}$, $1p_{3/2}$ and $1p_{1/2}$ shells of ^{16}O . If factorization were employed in the calculation, then the A_{TL} curves for the three shells will be identical to the free result. In the left panel we show results obtained when the enhancement of the lower components as well as the dispersive distortions of the spinor are removed. For these results factorization is only broken due to the spin-orbit coupling in the final state. In particular for the s -wave, factorization is fully recovered (factorization of the cross-section can be recovered if there is no spin-orbit in the final state and/or if the initial state is an s -state. This is due to the particular angular momentum algebra of the spin 1/2 final particle [26]). For the other two shells, only a modest deviation from the factorization approach is seen. This is typical for quasielastic kinematics.

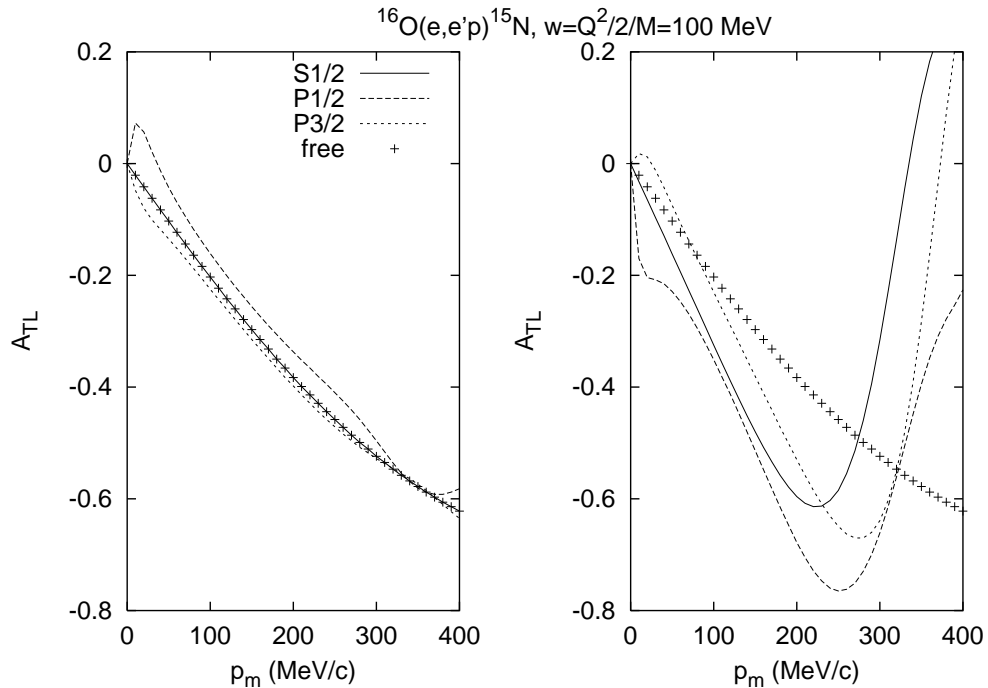


FIG. 5: Effect of the dynamical enhancement of the lower components observed in A_{TL} . In the right panel the dynamical enhancement as well as the dispersive distortion of the spinors is removed. The crosses show the free result, identical to the s -wave result in this approximation. In the left panel, the enhancement of the lower components and the dispersive distortion of the spinors is switched on. The departure from the factorized (free) result and the richer structure for the three shells is clearly seen. Note the tendency of the $j = \ell - 1/2$ spin-orbit partner to depart more from the free result[6, 25].

On the right panel, however, the whole calculation including the enhancement of the lower components is displayed. This shows a very visible departure from the factorized result for A_{TL} , with a much richer structure and a crossover of A_{TL} in between 200 and 300 MeV. This is a significant feature of A_{TL} that has been confirmed by experiment [2]. Also, the departure is larger for the $j = \ell - 1/2$ spin-orbit partner as predicted by the relativistic IA result [6, 25].

The important effect of the enhancement of the lower components in the A_{TL} observable would also be seen in the separate response R^{TL} and indeed this has been confirmed by experiments at $Q^2 = 0.8 \text{ (GeV/c)}^2$ [2]. We have then also compared the relativistic IA formalism to former results for R^{TL} obtained at moderate values of Q^2 (see Fig. 6) obtained at Saclay [27] and NIKHEF [28]. Though the enhancement of the lower components (present in the solid curves and removed in the dashed ones) does not show up as clearly in R^{TL} at these low Q^2 kinematics, the overall agreement of the relativistic IA result is better than that of the nonrelativistic analyses [28] (dotted curve in Fig 6).

3. SCALE FACTOR ANALYSES OVER A WIDE RANGE OF Q^2

Some recent works [29, 30] point to the possibility of a Q^2 dependence of the spectroscopic factor. For ^{16}O there are several $(e, e'p)$ experiments performed at different value of Q^2 , so it is a good nuclues to look for such effect. In Fig. 7, the scale factors needed to scale the theoretical RDWIA reduced cross-section to the experimental data are compared. Four sets of data points were

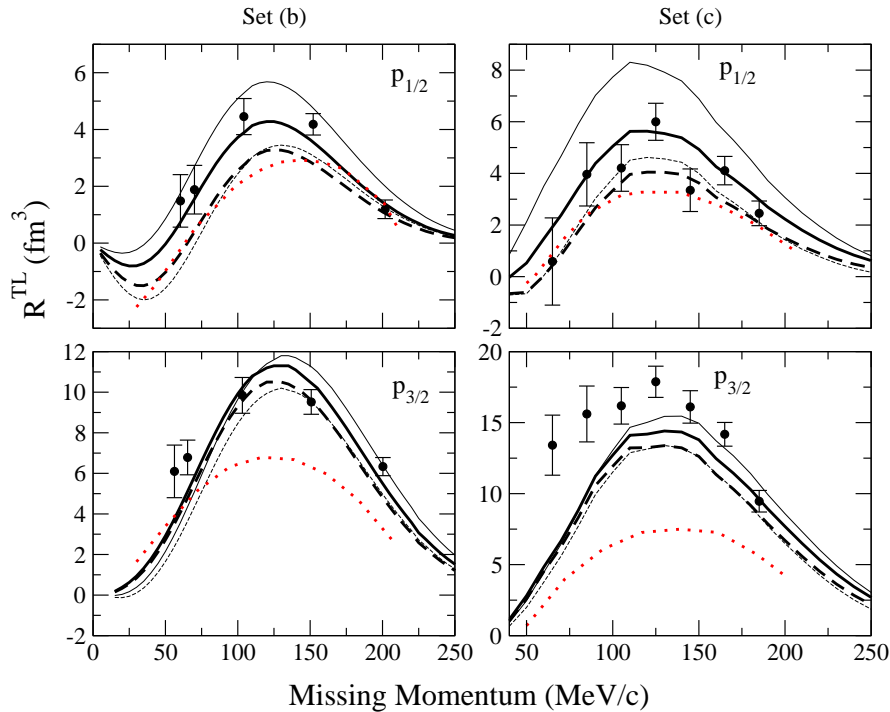


FIG. 6: TL responses compared to experimental data for $^{16}O(e, e'p)^{15}N$. Experiments from Spaltro et al. [28] (set (c), Q^2 of around $0.2 (GeV/c)^2$), and Chinitz et al. [27] (set (b), Q^2 of around $0.3 (GeV/c)^2$) Results with the current operator $cc1$ (thin lines) and $cc2$ (thick lines), Coulomb gauge, NLSH-P wave functions[33] and EDAI-O optical potential. Solid lines show the results of the full calculation, dashed lines the results without the dynamical enhancement of the lower components. Dotted lines show the result of the nonrelativistic analyses of ref. [28].

used, one in parallel kinematics from Leuschner *et al.* [31], and three in perpendicular kinematics (from refs. [2, 27, 28]).

We must note the following:

1. Scale factors are not independent on final state interactions (FSI). In particular, calculations with FSI based upon optical potentials fitted to elastic proton scattering in one hand, and upon the Glauber approach on the other, give generally different scale factors[30, 32]. This is due to the different picture of the FSI interaction assumed in each case. Which one is dominant in $(e, e'p)$ processes is yet to be known, and probably depend on the kinematics.

Also, as already said here, elastic proton data mainly constrain the asymptotic behaviour of the optical potentials. $(e, e'p)$ experiments are not very sensitive to this asymptotic or large r region, rather to the behaviour of the proton wave function (and thus the potential) in the inner nuclear region. This is the reason why optical potentials that yield essentially the same elastic (p, p) observables, can however lead to $(e, e'p)$ scale factors that differ by 50% or more [33]. In Fig. 7, the results shown in the left and right panels differ only in the relativistic optical potential employed. The effect on the scale factor is clearly visible while none of the two can be preferred over the other based upon elastic (p, p) scattering only. A very effective way of dealing with this optical potential uncertainty is to use also data from *inelastic* nucleon scattering, restricting thus more the potentials in the nuclear interior [34]. This is at the moment only available for nonrelativistic potentials in a restricted range of energies.

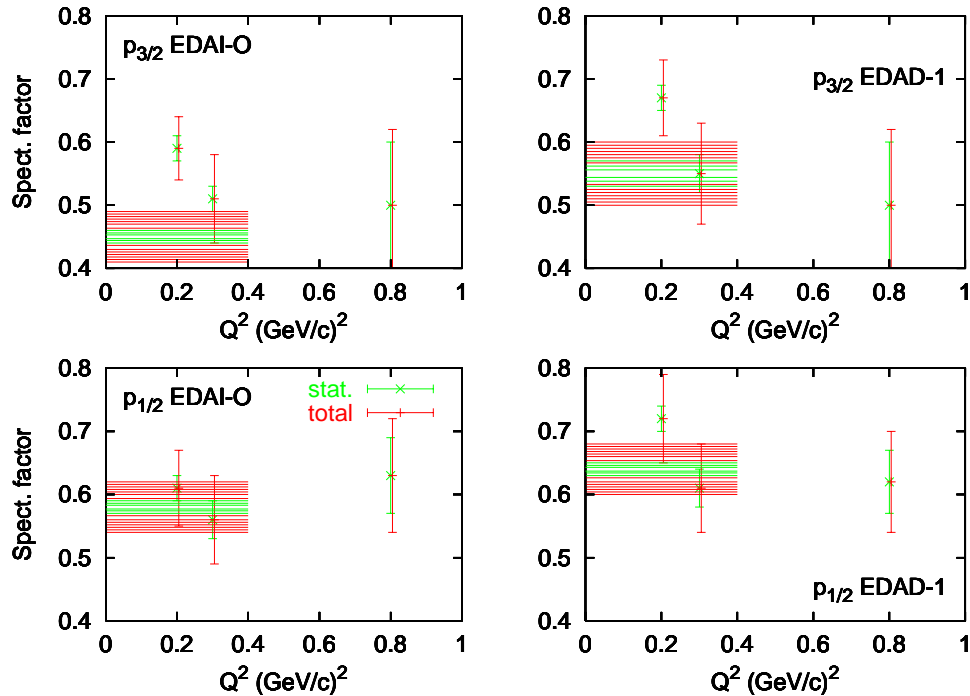


FIG. 7: Scale factors derived from experimental data for the valence states in $^{16}\text{O}(e, e'p)^{15}\text{N}$ at several Q^2 . Experiments from Leuschner et al. [31] (Q^2 range from 0 to 0.4 $(\text{GeV}/c)^2$, represented by the dashed area), Spaltro et al. [28] (Q^2 of around 0.2 $(\text{GeV}/c)^2$), Chinitz et al. [27] (Q^2 of around 0.3 $(\text{GeV}/c)^2$) and Gao et al. [2] (Q^2 of around 0.8 $(\text{GeV}/c)^2$) are shown. Results with the current operator $cc2$, Coulomb gauge, NLSH-P wave functions and EDAI-O (left) and EDAD-1 (right) potentials [33]. Statistical only and total uncertainty error bars are shown. Note that due to fragmentation, part of the $3/2^+$ strength is not included in the lowermost state here analyzed, what causes the scale factors for the $p_{3/2}$ shell to be smaller than for the $p_{1/2}$ one.

For a heavier nucleus as ^{208}Pb scale factors were much more stable against different choice of the optical potentials [3], mainly because all the available relativistic parametrizations were much more similar than for ^{16}O (compare left and right panel of Fig. 3).

2. Usually, lower Q^2 experiments span a smaller range in p_m than large Q^2 ones. Due to this, large Q^2 experiments give more weight to the large p_m region, where the IA is not the only prevailing reaction mechanism. Other contributions would naturally lead to an increase of the cross-section in the p_m region where the single-particle spectral function is not dominant, and thus fitting scale factors with data in this region will yield higher scale factors. When comparing data from experiments taken at different Q^2 in order to *deduce scale factors*, one should probably restrict oneself to those data in region of p_m where the IA result is important. So far this region is not well explored at high Q^2 for $^{16}\text{O}(e, e'p)^{15}\text{N}$, but new experiments at Jlab aiming at this will yield new high quality data very soon.

4. SUMMARY

In this contribution we have studied the differences between impulse approximation calculations for the $(e, e'p)$ reaction based upon the Schrödinger and Dirac equation. The overall good agreement

of the Dirac equation based results with experiment calls for a closer reexamination of the relativistic approach. While it is true that relativity should play a role in high Q^2 experiments, and thus a better agreement of the relativistic approach is expected from kinematical grounds, the fact that dynamical predictions of the single-particle relativistic picture, as for instance the richer structure of the A_{TL} asymmetry and the enhancement of the R^{TL} response are confirmed by the experiment needs further research where some approximations of the model (in particular its single-particle nature) could be removed.

ACKNOWLEDGMENTS

This work was partially supported under Contracts No. PB/98-1111, PB/98-0676, PB/96-0604 and by the Junta de Andalucía (Spain). J.R.V. and A.E. acknowledge support from doctoral fellowships of the Consejería de Educación de la Comunidad de Madrid and Ministerio de Educación y Cultura (Spain), respectively.

REFERENCES

- [1] S. Boffi, C. Giusti, F.D. Pacati, Phys. Rep. **226**, 1 (1993); S. Boffi, C. Giusti, F. Pacati, M. Radici, “*Electromagnetic Response of Atomic Nuclei*”, (Oxford-Clarendon Press, 1996); J.J. Kelly, Adv. Nucl. Phys. **23**, 75 (1996).
- [2] J. Gao *et al.*, Phys. Rev. Lett. **84**, 3265 (2000).
- [3] J.M. Udías, P. Sarriguren, E. Moya de Guerra, E. Garrido, J.A. Caballero, Phys. Rev. C **48**, 2731 (1993).
- [4] J.M. Udías, P. Sarriguren, E. Moya de Guerra, E. Garrido, J.A. Caballero, Phys. Rev. C **51**, 3246 (1995).
- [5] J.M. Udías, P. Sarriguren, E. Moya de Guerra, J.A. Caballero, Phys. Rev. C **53**, R1488 (1996).
- [6] J.M. Udías, J.A. Caballero, E. Moya de Guerra, J.E. Amaro, T.W. Donnelly, Phys. Rev. Lett. **83**, 5451 (1999).
- [7] A. Picklesimer, J.W. Van Orden, Phys. Rev. C **35**, 266 (1987); **40**, 290 (1989).
- [8] Y. Jin, D.S. Onley, Phys. Rev. C **50**, 377 (1994).
- [9] S.Gardner, J.Piekarewicz, Phys.Rev. C **50**, 2882 (1994).
- [10] C.J. Horowitz, D.P. Murdock, B.D. Serot, *Computational Nuclear Physics*, Eds. K. Langanke, J.A. Maruhn, S.E. Koonin (Springer, Berlin, 1991).
- [11] E.D. Cooper, S. Hama, B.C. Clark, R.L. Mercer, Phys. Rev. C **47**, 297 (1993).
- [12] J.E. Amaro, J.A. Caballero, T.W. Donnelly, A.M. Lallena, E. Moya de Guerra, J.M. Udías, Nucl. Phys. **A602**, 263 (1996); J.E. Amaro, J.A. Caballero, T.W. Donnelly, E. Moya de Guerra, **A611**, 163 (1996).
- [13] S. Jeschonnek, T.W. Donnelly, Phys. Rev. C **57**, 2438 (1998); S. Jeschonnek, Phys. Rev. C **63**, 034609 (2001); S. Jeschonnek, J.W. Van Orden, Phys. Rev. C **62**, 044613 (2000).
- [14] T. de Forest, Nucl. Phys. **A392**, 232 (1983).
- [15] C. Giusti, F. Pacati, Nucl. Phys. **A473**, 717 (1987).
- [16] E. Quint, Ph.D. thesis, University of Amsterdam (*unpublished*) (1988).
- [17] A. Meucci, C. Giusti and F. Pacatti, Phys. Rev. C **64** 014604 (2001).
- [18] J.J. Kelly, Phys. Rev. C **56**, 2672 (1997); **59**, 3256 (1999).
- [19] G.H. Rawitscher, Phys. Rev. C **31**, 1173 (1985).
- [20] F.G. Perey and B. Buck, Nucl. Phys. **A2**, 353 (1962); H. Fiedeldey, *ibid.* **77**, 149 (1966).
- [21] M.M. Giannini and G. Ricco, Ann. Phys. (N.Y.) **102**, 458 (1976).
- [22] P. Schwandt, H.O. Meyer, W.W. Jacobs, A.D. Bacher, S.E. Vigdor, M.D. Kaitchuck, T.R. Donoghue, Phys. Rev. C **26**, 55 (1982).
- [23] S. Boffi, C. Giusti, F.D. Pacati, F. Cannata, Nuovo Cimento **98**, 291 (1987).
- [24] J.A. Caballero, T.W. Donnelly, E. Moya de Guerra, J.M. Udías, Nucl. Phys. **A632**, 323 (1998).
- [25] J.A. Caballero, T.W. Donnelly, E. Moya de Guerra, J.M. Udías, Nucl. Phys. **A643**, 189 (1998).
- [26] J.A. Caballero, Ph.D. Thesis, Universidad Autónoma de Madrid (1991) *unpublished*.
- [27] L. Chinitz *et al.*, Phys. Rev. Lett. **67**, 568 (1991).

- [28] C.M. Spaltro, H.P. Blok, E. Jans, L. Lapikás, M. van der Schaar, G. van der Steenhoven, P.K.A. de Witt Huberts, Phys. Rev. C **48**, 2385 (1993).
- [29] L. Frankfurt, M. Strikman and M. Zhalov, Phys. Lett. **B503** 73 (2001).
- [30] L. Lapikas, G. van der Steenhoven, L. Frankfurt, M. Strikman, M. Zhalov Phys. Rev. C **61** 064325 (2000).
- [31] M. Leuschner *et al.*, Phys. Rev. C **49**, 955 (1994).
- [32] D. Debruyne, J. Ryckebusch, in “Proceedings of the Third International Conference on Perspectives in Hadronic Physics (Trieste, 2001)”, *in press*.
- [33] J.M. Udias, J.A. Caballero, E. Moya de Guerra, Javier R. Vignote, A. Escuderos, Phys. Rev. C **64**, 024614 (2001).
- [34] J.J. Kelly *et al.*, Phys. Rev. C **39**, 1222 (1989); J.J. Kelly, Phys. Rev. C **39**, 2120 (1989); J.J. Kelly *et al.* Phys. Rev. C **41**, 2504 (1990); Q. Cheng, J.J. Kelly, P.P. Singh, M.C. Radhakrishna, W. P. Jones and H. Nann, Phys. Rev. C **41**, 2514 (1990); R.S. Flanders *et al.*, Phys. Rev. C **43**, 2103 (1991).